[Journal of Geophysical Research - Atmospheres]

Supporting Information for

Spatiotemporal Hysteresis Distribution and Decomposition of Solar Activities and Climatic Oscillation during 1900–2020

Mingyang Li[1], Tingxi Liu[1,*], Long Ma[1,*], Limin Duan[1], Yixuan Wang[1], Guoqiang Wang[2], Huimin Lei[3], Vijay Singh[4]

[1] Inner Mongolia Water Resource Protection and Utilization Key Laboratory; Water Conservancy and Civil Engineering College, Inner Mongolia Agricultural University, Hohhot 010018, China;

[2] College of Water Sciences, Beijing Normal University, Beijing 100875, China;

[3] State Key Laboratory of Hydroscience and Engineering, Department of Hydraulic Engineering,

Tsinghua University, Beijing 100084, China;

[4] Department of Biological and Agricultural Engineering & Zachry Department of Civil Engineering, Texas A& M University, College Station, TX 77843, USA).

Contents of this file

Introduction

In the "sun-climate-water resource" system, meteorological elements have different lag periods for influence factors such as solar activity (SA), climate oscillation (CO) and geographical factors (GF) at different spatiotemporal scales. However, this phenomenon has been insufficiently investigated. It is unclear whether the strong interaction/lag behaviours of meteorological elements responses to SA/CO that were calculated, statistically true and realistically possible. There is also insufficient information regarding the reasons and their weights for lag variation in different regions. Moreover, the transmission mechanism of the lag is also unclear. To overcome this knowledge gap, we studied temperature (T) and precipitation (P) data collected over 121 years from 3,836 grid stations across China. The spatial distribution of T and P, strong interaction periodic distribution responses to SA and CO, and hysteresis distribution were studied under six periodic scales (0–5, 5–10, 10–30, 30–60, 60–90, and 90–120 a), the. The weight distribution of lag influencing factors was plotted using false colour RGB to represent SA, GF, and CO; a multivariate hysteresis decomposition model was proposed to simulate and quantitatively decompose the periodic lag considering the factors of the earth's revolution.

We found that the strong interaction/lag period obtained on a long-time scale can be decomposed into several short, strong interaction/lag periods which are shorter than the SA period (11.2 a). The distribution of strong interaction and lag period is nested with the terrain and varies with the city. Additionally, regional underlying surface conditions and urbanisation significantly affect the lag periods of T and P.

There are two distinct dividing lines for the lag periods of T and P and patterns of influencing factors. The dividing lines for T run through valleys where water veins or mountains meet and gaps facilitate the cross-regional flow of monsoons. The two dividing lines are the Central Gobi–Ordos Plateau–Hengshan–Yanshan and the southern foot of the northern Tibetan Plateau–Cherchen River–Turpan Basin. The dividing line for P runs through the region where terrain changes drastically. Tall mountains of the Greater Hinggan–Taihang–Wushan–Xuefeng Mountains and Qilian–Bayankela–Hengduan Mountains block water vapour transportation. Regarding T lag trends, the northern region of China displays the longest lag period; the lag period of surrounding regions tends to converge toward the northern region. The lag period caused by sunspot numbers (SN) in Southwest China is larger than that in Northwest China, while the hysteresis effect of CO is opposite in the two regions. The hysteresis trend of P also has similar characteristics; the difference is that central China has the longest lag period.

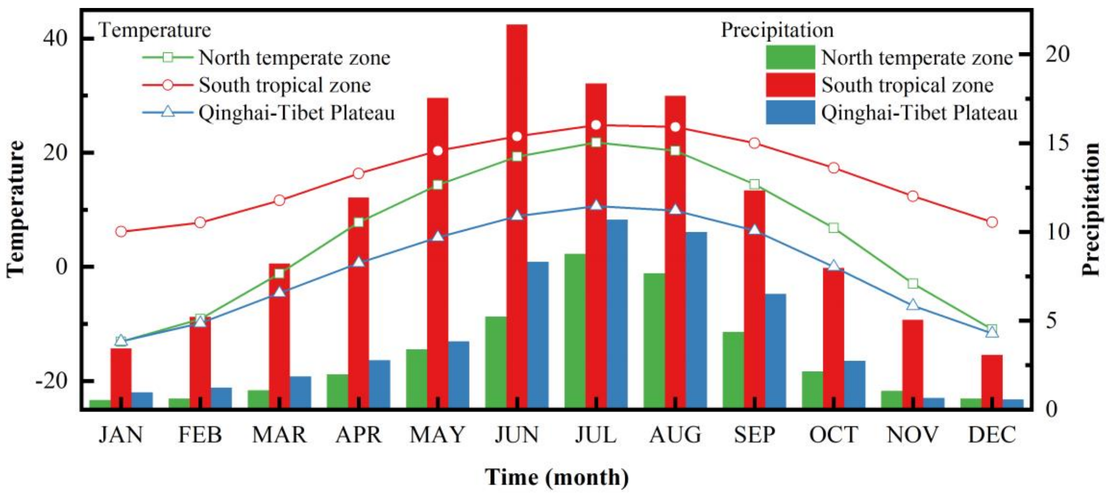

Figure S1. Plot showing T and P in north temperate zone, south tropical zone and Qinghai-Tibet plateau of China for the period 1900 to 2020.

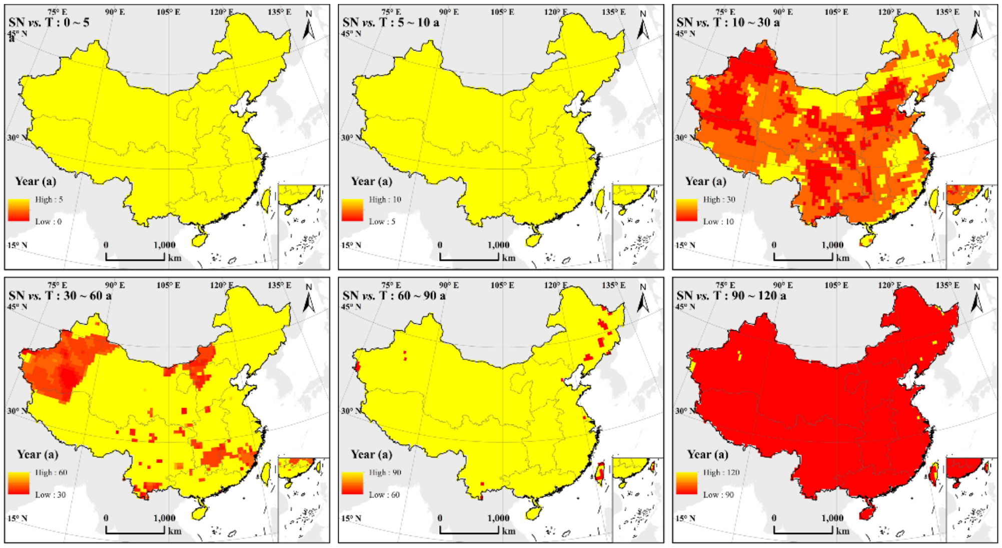
SN vs. T : 0 ~ 5 a
SN vs. T : 5 ~ 10 a
SN vs. T : 10 ~ 30 a
SN vs. T : 30 ~ 60 a
SN vs. T : 60 ~ 90 a
SN vs. T : 90 ~ 120 a
Year (a)
High : 5
Low : 0
High : 10
Low : 5
High : 30
Low : 10
High : 60
Low : 30
High : 90
Low : 60
High : 120
Low : 90
75° E
90° E
105° E
120° E
135° E
45° N
30° N
15° N
N
0
1,000
km

(a)

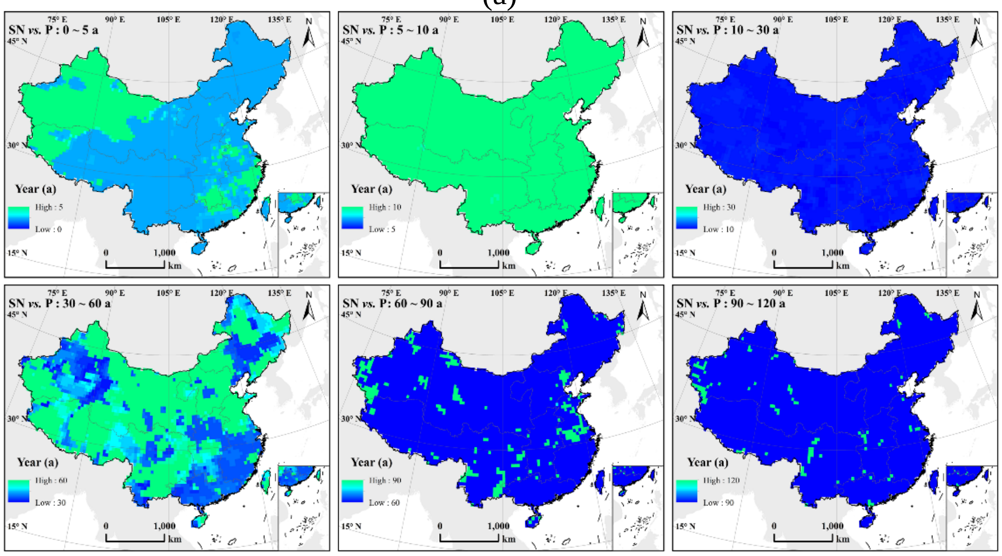
SN vs. P : 0 ~ 5 a
SN vs. P : 5 ~ 10 a
SN vs. P : 10 ~ 30 a
SN vs. P : 30 ~ 60 a
SN vs. P: 60 ~ 90 a
SN vs. P : 90 ~ 120 a
Year (a)
High : 5
Low : 0
High : 10
Low : 5
High : 30
Low : 10
High : 60
Low : 30
High : 90
Low : 60
High : 120
Low : 90
75° E
90° E
105° E
120° E
135° E
45° N
30° N
15° N
N
0
1,000
km

(b)

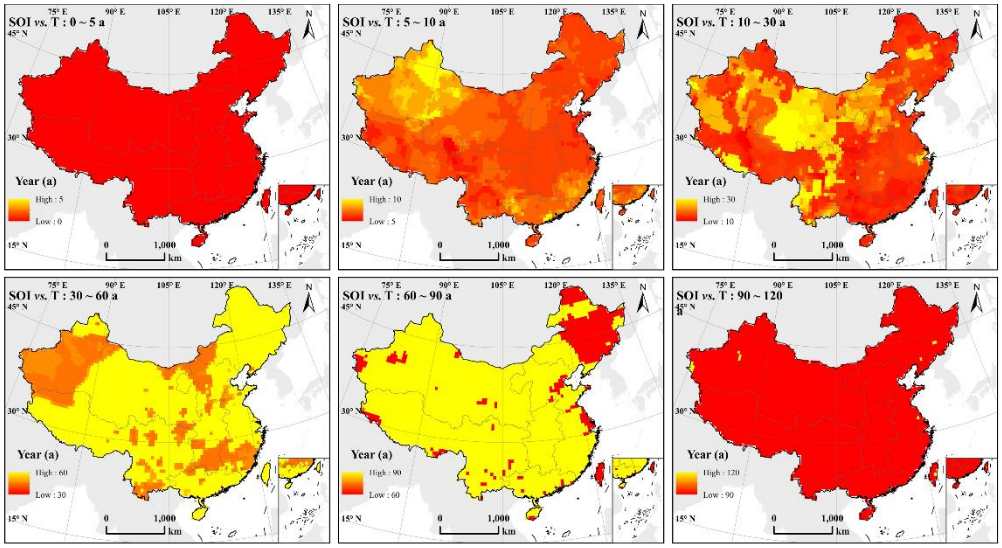
SOI vs. T : 0 ~ 5 a
SOI vs. T : 5 ~ 10 a
SOI vs. T : 10 ~ 30 a
SOI vs. T : 30 ~ 60 a
SOI vs. T : 60 ~ 90 a
SOI vs. T : 90 ~ 120 a
Year (a)

(c)

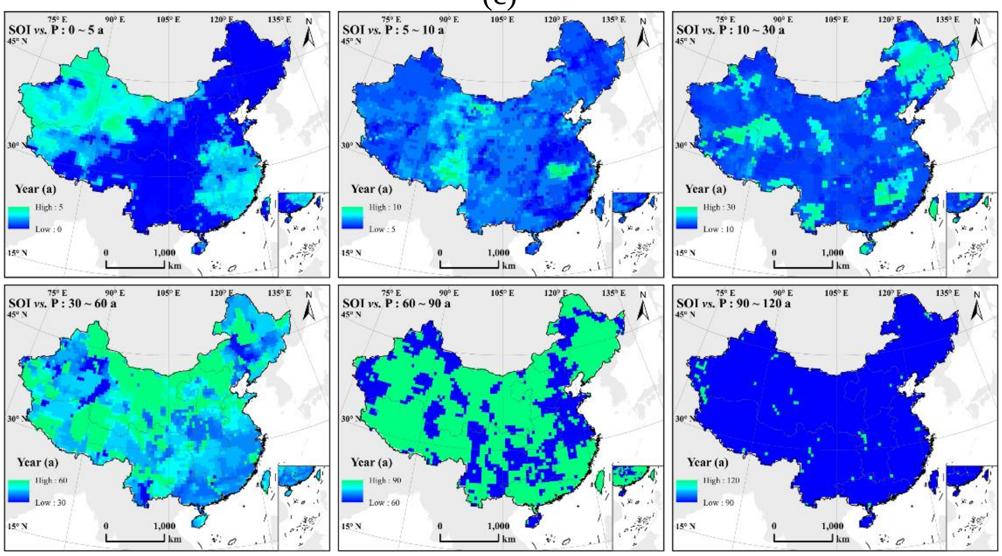
SOI vs. P : 0 ~ 5 a
SOI vs. P : 5 ~ 10 a
SOI vs. P : 10 ~ 30 a
SOI vs. P : 30 ~ 60 a
SOI vs. P : 60 ~ 90 a
SOI vs. P : 90 ~ 120 a
Year (a)

(d)

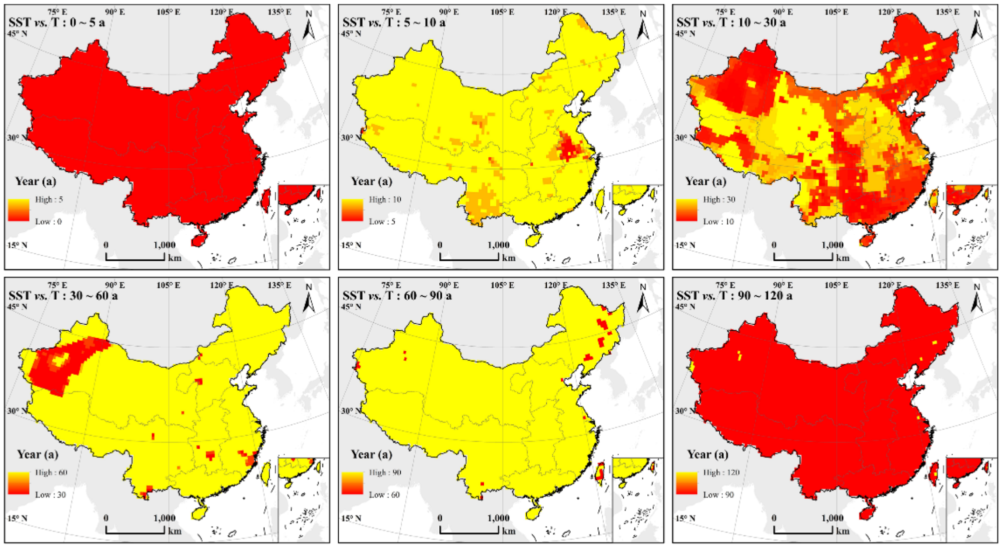

(e)

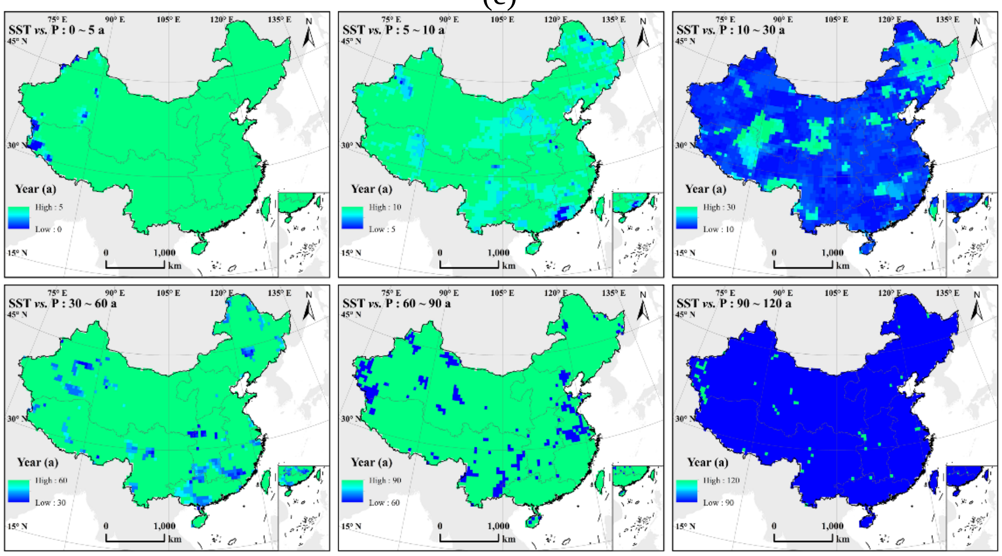

(f)

Figure S2. The significant periodic distributions of SN, SOI and SST to T (a, c, e) and P (b, d, f) of China under six periodic scales (The significance level = 0.95).

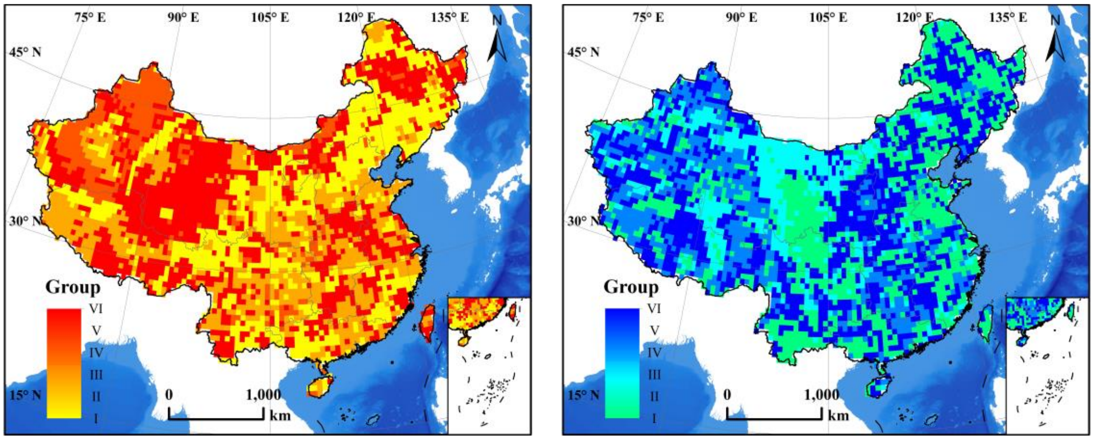

(a) (b)

Figure S3. The hysteresis grouping distribution of T (a) and P (b) related to SA, CO, and GF of China using entropy weight under six periodic scales.